Low-energy ion neutralization at surfaces: Resonant and Auger processes

N. P. Wang,* Evelina A. García, R. Monreal, and F. Flores
Departamento de Física Teórica de la Materia Condensada, C-V, Universidad Autónoma de Madrid, E-28049 Madrid, Spain

E. C. Goldberg
Instituto de Desarrollo Tecnológico para la Industria Química (CONICET-UNL), Güemes 3450, CC91, 3000, Santa Fe, Argentina

H. H. Brongersma
Department of Physics, Eindhoven Technical University, P.O. Box 513, NL-5600 Eindhoven, The Netherlands

P. Bauer
Institut für Experimentalphysik, Johannes-Kepler Universität Linz, A-4040 Linz, Austria
and Donostia International Physical Center, San Sebastián, Spain
(Received 20 December 2000; published 30 May 2001)

The interaction of He^+ with a typical metal surface (Al or Pd) is described, analyzing in detail the different mechanisms that contribute to the neutralization of the projectile when backscattered from the surface. Auger and resonant neutralization processes are considered and analyzed including a detailed quantum-mechanical description of the He-metal interaction, for projectile energies between 100 eV and 3 keV. We show that the promotion of the He-1*s* level, due to its interaction with the metal-atom-core orbitals, is the crucial mechanism making resonant processes operative. We find, however, that resonant processes are much more important for Al than for Pd. In Al, both Auger and resonant processes are equally important for neutralization of the ion, while for Pd we find that Auger is the dominant mechanism, making the He/Pd system the ideal case for which Hagstrum's exponential law appears to be practically valid for all velocities. We also find qualitative agreement with experimental data, which we consider a satisfactory result in view of the fact that our theory is a complex *ab initio* calculation free of adjustable parameters.

DOI: 10.1103/PhysRevA.64.012901 PACS number(s): 34.50.Dy, 79.20.Rf

I. INTRODUCTION

Low energy ion scattering (LEIS) is a widely used surface-analysis technique to obtain information on the composition and the structure of a surface. In LEIS, the surface under investigation is bombarded by He^+ ions with a kinetic energy of $\approx$1 keV at a large angle with respect to the surface. The surface composition is obtained from the energy spectrum of ions that are backscattered by a large angle (typically 135°). Amongst the backscattered projectiles, only a fraction P^+ leaves the surface as a (singly charged) positive ion. The main advantages of LEIS are (i) its extreme surface sensitivity (LEIS is sensitive just to the outermost layer, since ions that are backscattered from deeper layers are very efficiently neutralized) and (ii) its insensitivity to the local (chemical) environment of the backscattering atom (i.e., generally no matrix effects are observed) [1].

The main objective of this paper is to describe the interaction of He^+ with a typical metal surface (we will consider either Al or Pd) and analyze in detail the different mechanisms that contribute to the neutralization of the projectiles when backscattered from a surface atom. In the literature, neutralization processes have mostly been analyzed by considering either Auger or resonant neutralization independently. Hagstrum's Auger neutralization (AN) model dates back to 1954 [2] and was developed to describe ion neutralization at very low velocities, i.e., for ion velocities small compared to the target Fermi velocity, a condition also met in LEIS. In Hagstrum's theory the fraction of ions that are not neutralized along the incoming (or outgoing) trajectory is given by $P^+ = \exp(-v_c/v_\perp)$, where v_c is a characteristic velocity of the metal and $v_\perp$ is the perpendicular component of the ion velocity with respect to the surface. We will see below how Hagstrum's model has to be modified in order to include neutralization due to resonant processes. The relevance of resonant processes (resonant neutralization and resonant ionization) has been investigated by many authors [3–7]. In resonant neutralization (RN) the empty-ion energy level is resonating with the occupied part of the metal conduction band and a metal electron is transferred to the ion; in resonant ionization, the empty levels of the metal conduction band resonate with the ion energy level and electron tunneling occurs in the opposite direction. Our main goal is to combine all these processes (Auger and Resonant) into a unified model for ion neutralization, to find out which processes are dominant in the different regions of ion energies. At the same time, we want to understand which conditions have to be met in order to make Hagstrum's exponential law still applicable, and how v_c is related to other metal properties.

II. MODEL AND GENERAL SOLUTION

A. Ion trajectory and He^+-metal interaction potential

The incoming ion follows a trajectory perpendicular to the surface and directed towards a surface atom while the out-

*On leave from Fudan University, Shanghai, People's Republic of China.

going species (either He^+ or He^0) are scattered off at an angle of 45° with respect to the surface (corresponding to a scattering angle of 135°).

At long distances the ion feels an image potential (see below), while at very short distances the ion and the metal atom undergo a binary collision. For the case of $^4He^+$ backscattered at 135°, the velocities of the scattered He ion and of the recoiling metal atom are, in the laboratory frame, $v_{\mathrm{Al}}=0.24v_{in}$ and $v_{out}=0.78v_{in}$ for He/Al and $v_{\mathrm{Pd}}=0.07v_{in}$ and $v_{out}=0.94v_{in}$ for He/Pd, v_{in} being the incoming velocity of He. In our description of resonant processes we neglect the recoil of the metal atom, since—due to their low velocity—they travel only a short distance during the time interval when resonant processes are operative, i.e., ca. 0.5 a.u.

There is also—apart from the close collision—a change of the ion velocity along the trajectory due to its interaction with the metal (which corresponds to the image potential at large distances). We accounted for this effect in our calculation and found no significant change in the results. Thus, in this article we will assume the ion to be backscattered at the turning point of the trajectory with an outgoing velocity equal to the incoming one; in this way we maintain the relative velocity between projectile and scattering center.

B. Ion neutralization. Resonant and Auger processes

In our approach to investigate the charge-transfer processes between He^+ and a metal, we distinguish between Auger and resonant processes since these processes act in different spatial regions: AN acts at large distances, while resonant processes act only during the close collision (see below for a discussion of this approximation). Note that during the close collision also AN will be active, but with much lower transition rates as compared to RN and may therefore be safely neglected there.

With these assumptions we calculate independently the Auger survival probabilities for the incoming and outgoing paths, $P^+_{A,in}$ and $P^+_{A,out}$, respectively, as well as the probabilities for He^+ to survive and He^0 to be reionized in the close collision P^+_{surv} and P_{reion}, respectively. From these quantities we obtain the total ion fraction after the whole ion-surface interaction, P^+, by means of the following equation:

$$P^+=P^+_{A,in}P^+_{surv}P^+_{A,out}+(1-P^+_{A,in})P_{reion}P^+_{A,out}. \quad (1)$$

In the following, we will refer to the first and second parts of Eq. (1) as the survival channel and the reionization channel, respectively. In the reionization channel, a contribution to P^+ is obtained from the ions Auger neutralized along the incoming trajectory due to the resonant-ionization mechanism. Next we discuss how to calculate the different quantities appearing in Eq. (1). Atomic units ($e=\hbar=m=1$) are used throughout this work.

III. RESONANT PROCESSES

A. General formalism

For the He-metal system, resonant processes are due to charge transfer between the He-1s level and the metal valence electrons. In this context, the promotion of the He-1s level due to its interaction with the metal-core electrons is important, due to which the He-1s level may become resonant with the metal conduction band so that resonant processes become very efficient [8,9]. Therefore it is very important to calculate carefully the position of the He-1s level as a function of He-metal distance.

In our approach to this problem, we follow Ref. [7] and describe the interaction between the He-1s level and the metal by means of the Linear Combination of Atomic Orbitals (LCAO) approach using a molecular-orbital basis. As relevant levels we include the following orbitals: He 1s; Al 2s, 2p, 3s, and 3p; and Pd 3s, 3p, 3d, 4s, 4p, 4d, and 5s. All the other core levels (Al 1s and Pd 1s, 2s, 2p) are included in the calculation using a pseudopotential technique, equivalent to analyzing the different interatomic orbital interactions by means of a second-order overlap expansion, which implies having very small overlap between the core levels and the He-1s orbital.

In our LCAO approach we first calculate the different interactions between the He-1s level and the metal orbitals using quantum chemistry techniques, then, we analyze the chemisorption energy for different cases: in the first configuration, we consider He^+ as a frozen charge state and assume, to be consistent, all the hopping parameters $T_{1s,i}$ between the He-1s level and the metal orbital i to be zero. In the second configuration we consider frozen He^0 assuming $T_{1s,i}=0$. We define the ''diabatic'' He-1s level, $\tilde{E}_{1s}$, as the energy difference of the total system for the charge states He^0 and He^+, $E[He^+]$ and $E[He^0]$ with respect to the Fermi level E_F,

$$E[He^0]-E[He^+]=\tilde{E}_{1s}-E_F. \quad (2)$$

Note that the difference $E[He^+]-E[He^0]$ measures the change in potential energy of the ion when going from the He^+ to the He^0 state (see Ref. [10] for details).

In the next step we define an effective spinless Newns-Anderson Hamiltonian where we introduce the diabatic $\tilde{E}_{1s}$ level of He and the hopping terms $T_{1s,i}$ that have been neglected in the previous step. This Hamiltonian reads

$$\hat{H}=\tilde{E}_{1s}(\mathbf{R})\hat{n}_{1s}+\sum_i \epsilon_i\hat{n}_i+\sum_i [T_{1s,i}\hat{c}^\dagger_{1s}\hat{c}_i+\mathrm{H.c.}] + \sum_{i\neq j}[T_{i,j}\hat{c}^\dagger_i\hat{c}_j+\mathrm{H.c.}], \quad (3)$$

where the unperturbed eigen values ϵ_i and the hopping integrals $T_{i,j}$ are the LCAO parameters associated with the free orbitals of the crystal and with the corresponding electronic structure. The Newns-Anderson Hamiltonian is usually written in a momentum representation [3,4], which is straightforwardly obtained from Eq. (3) by changing to the basis of Bloch wave functions giving the electronic structure of the metal. The Al and Pd surfaces are assumed to be unreconstructed and have fcc (111) symmetry. The tight-binding parameters for Al and Pd are taken from Ref. [11]. Different integrals needed to obtain the hopping between He and the

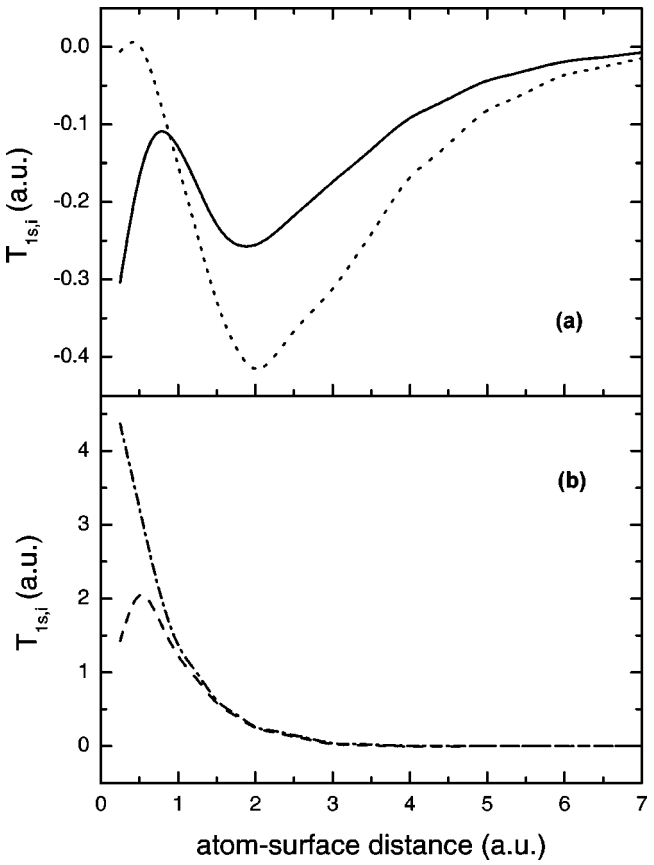

FIG. 1. The hopping parameters $T_{1s,i}$ for the He-1s level and different atomic orbitals of Al. (a) $i=3s$ (continuous line) and $i=3p_z$ (dotted line). (b) $i=2s$ (dot-dashed line) and $i=2p_z$ (dashed line). Distances are measured with respect to the first atomic layer.

metal surfaces are calculated using Slater single-ζ orbitals [12] and the code of Refs. [13,14]. The excited states $2\,^1S$ and $2\,^3S$ of He in front of an Al surface have also been analyzed in Ref. [10] and their contribution to the neutralization of He^+ was found to be small. The reason is that these excited states are above the Fermi level in the range of distances of interest. Therefore, they will be neglected in this work.

B. $\tilde{E}_{1s}$ and $T_{1s,i}$ for He/Al and He/Pd

Figure 1 shows $T_{1s,i}$, where i stands for the $2s$, $2p$, $3s$, and $3p$ orbital of Al, as a function of the metal-He distance along the direction perpendicular to the surface. Zero distance corresponds to the metal atom center.

Figure 2 shows $\tilde{E}_{1s}$ for the He/Al system. The $\tilde{E}_{1s}$ level is obtained from Eq. (2) when $E[\mathrm{He}^0]$ and $E[\mathrm{He}^+]$ are known. These quantities have already been calculated for Al in Ref. [10] for distances between 1 and 10 a.u. The values of $\tilde{E}_{1s}$ given in Fig. 2 are also similar to the ones published in Ref. [10], but our values are more accurate, since the Al-2s orbital and the 1s-core level are included in our calculation. At large distances we recover the image potential limit, while at small distances $\tilde{E}_{1s}$ bends down, basically due to electrostatic interaction between the He-1s level and the Al atomic

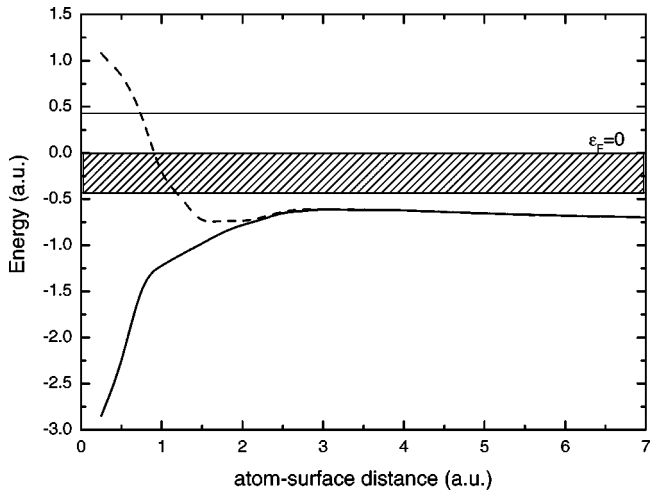

FIG. 2. The adiabatic energy level of He, E_{1s}, in front of Al (dashed line) is shown together with the diabatic level, $\tilde{E}_{1s}$, (continuous line). The top and the bottom of the conduction band of Al are schematically drawn as two horizontal straight lines. The zero of energy is taken at the Fermi level so that the hatched region represents the occupied part of the band. Due to the interaction between He and the core electrons of Al, the He-1s level is promoted and resonates with the conduction band close to the surface.

charge. In Fig. 2 we also show the adiabatic level E_{1s}, which is the molecular orbital level resulting from the interaction between $\tilde{E}_{1s}$ and the Al-core orbitals. Note that at large distances both energy levels coincide, while at small distances the hopping integrals $T_{1s,i}$ modify $\tilde{E}_{1s}$ substantially by promotion of the He-1s level, so that for small distances this new level overlaps with the conduction band of Al.

Figure 3 gives $T_{1s,i}$ for the He/Pd system, where i stands for the $3s$, $3p$, $3d$, $4s$, $4p$, $4d$, and $5s$ orbital of Pd.

Figure 4 shows $\tilde{E}_{1s}$ and the adiabatic level E_{1s} for the He/Pd system. The behavior of $\tilde{E}_{1s}$ is similar to the one found for Al. Note again the promotion of the He-1s level and its overlap with the Pd conduction band, due to hopping.

C. Dynamic solution of the Newns-Anderson Hamiltonian

The time-dependent evolution of the He-1s level occupation number $n_{1s}(t)$ has been analyzed using Keldysh-Green function techniques [15]. Details have been published elsewhere [7]; let us only summarize here that in this approach we calculate the Green function $G^r_{1s,1s}(t,t')$ associated with the He-1s level. This Green function satisfies the following integrodifferential equation:

$$
\begin{aligned}
&i dG^r_{1s,1s}(t,t')/dt - \tilde{E}_{1s}(\mathbf{R}(t))G^r_{1s,1s}(t,t') \\
&\quad = \delta(t-t') + \int_{t'}^{t} dt_1\, \Sigma^r_{1s,1s}[\mathbf{R}(t),\mathbf{R}(t_1);t,t_1] \\
&\qquad \times G^r_{1s,1s}(t_1,t'), \qquad (4)
\end{aligned}
$$

where the self-energy $\Sigma^r_{1s,1s}$ is given by

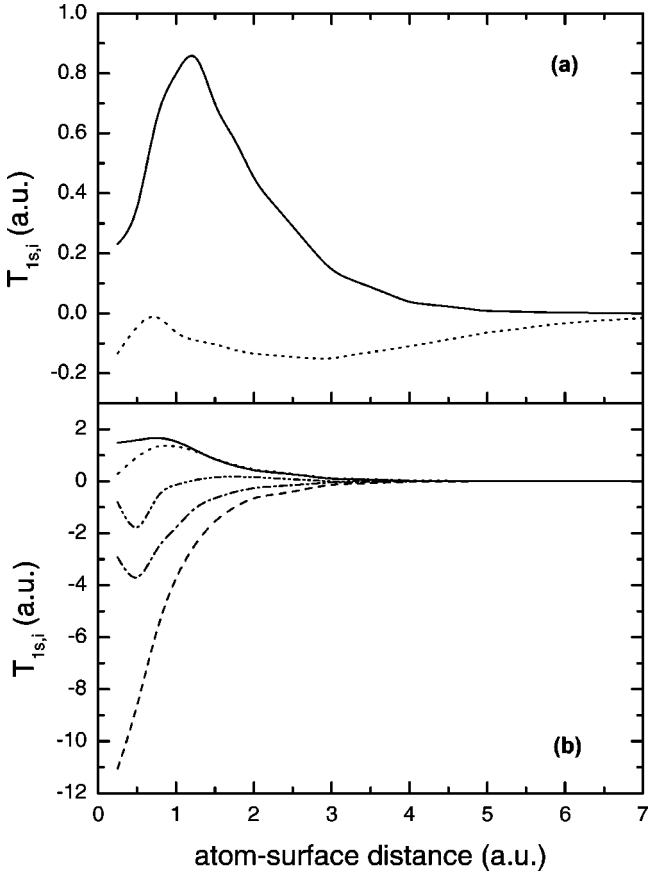

FIG. 3. The hopping parameters $T_{1s,i}$ for the He-1s level and different atomic orbitals of Pd. (a) $i=4d_{z^2}$ (continuous line) and $i=5s$ (dotted line). (b) $i=4s$ (continuous line), $i=4p_z$ (dashed line), $i=3d_{z^2}$ (dashed-double dotted line), $i=3p_z$ (dot-dashed line), and $i=3s$ (long-dashed line).

$$\Sigma^r_{1s,1s}[\mathbf{R}(t),\mathbf{R}(t_1);t,t_1] = \int_{-\infty}^{+\infty}\frac{d\omega}{2\pi}\Theta(t-t_1)e^{-i\omega(t-t_1)} \times\sum_{i,j} T_{1s,i}(\mathbf{R}(t))g^r_{i,j}(\omega)T_{j,1s}(\mathbf{R}(t_1)), \quad (5)$$

$g^r_{i,j}(\omega)$ being the retarded Green function of the unperturbed metal surface. In Eqs. (4) and (5) $\tilde{E}_{1s}$, and $T_{1s,i}$ depend on the time-dependent ion position $\mathbf{R}(t)$. Once we calculate $G^r_{1s,1s}(t,t')$, the occupancy $n_{1s}(t)$ is obtained from the equation

$$n_{1s}(t)=n_{1s}(t_0)|G^r_{1s,1s}(t,t_0)|^2+\sum_{i,j}\int_{-\infty}^{+\infty}d\omega\, n_F(\omega)\rho_{i,j}(\omega) \times\int_{t_0}^{t}dt_1\, G^r_{1s,1s}(t,t_1)T_{1s,i}(\mathbf{R}(t_1)) \times\int_{t_0}^{t}dt_2\, G^{r*}_{1s,1s}(t,t_2)T_{1s,i}(\mathbf{R}(t_2))e^{-i\omega(t_1-t_2)}, \quad (6)$$

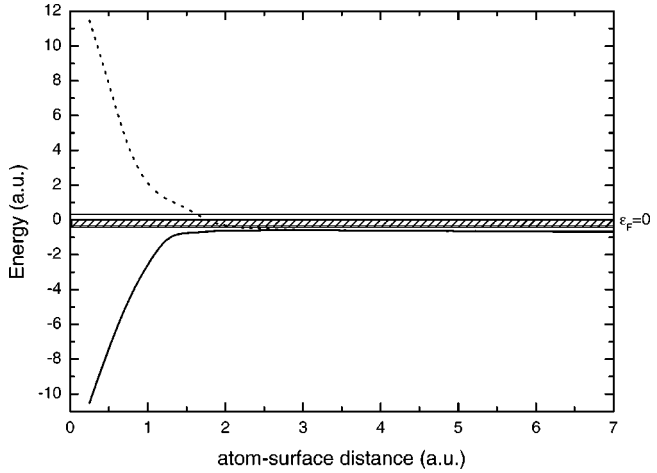

FIG. 4. The same as Fig. 2 but for Pd.

where $n_F(\omega)$ is the Fermi-Dirac distribution function of the metal electrons and $\rho_{i,j}(\omega)$ the density matrix for the metal surface,

$$\rho_{i,j}(\omega)=-\frac{1}{\pi}\mathrm{Im}\, g^r_{i,j}(\omega). \quad (7)$$

In Eq. (6), t_0 is the initial time used to solve numerically Eqs. (4) and (6) with the initial conditions $n_{1s}(t_0)=0$ for incident ions and $n_{1s}(t_0)=1$ for incident neutral atoms. The initial condition $n_{1s}(t_0)=0$ is used to calculate P^+_{surv} while $n_{1s}(t_0)=1$ is used to calculate P_{reion}. The initial time is defined by an initial distance d_0 large enough (d_0 around 7 a.u. from the last metal layer).

IV. AUGER PROCESSES

In our basic Eq. (1) we have assumed that resonant and Auger processes are spatially separated. From the results presented in Figs. 2 and 4 we can conclude that this is a good approximation. In these figures we see that the adiabatic He-1s level E_{1s} is below the metal conduction band for large distances so that only Auger neutralization can operate there. When E_{1s} resonates with the conduction band, Auger processes can still operate but their rate is small in comparison with that of resonant processes and can be neglected. With these assumptions we can consider Auger and resonant processes as spatially separated and, consequently, we will define the separation point z_s as the distance where E_{1s} crosses the bottom of the metal conduction band. Since Auger processes are important for distances larger than $z_s\sim 1$ a.u., we will use the jellium model to describe these processes. Note that, when the distance between atom and surface increases, more and more metal atoms contribute to Auger neutralization and the use of the jellium model becomes more appropriate.

In contrast to resonant processes, Auger processes will be treated semiclassically here. In the semiclassical approximation (SCA) the transition rates for capture ($1/\tau_{AC}$) or loss ($1/\tau_{AL}$) of an electron by the ion is calculated quantum mechanically, using Fermi's golden rule, as a function of dis-

tance. These rates are then inserted into a classical (master) equation giving the instantaneous occupancy of the atomic orbital. Within this approximation, and taking into account that no loss process is possible when the ion energy level is below the Fermi level at the low velocities considered in this work, the Auger survival probability for the incoming trajectory reads

$$P^{+}_{A,in} = \exp\left[-\frac{1}{v_{in\perp}} \int_{z_s}^{\infty} dz \, \frac{1}{\tau_{AC}(z)} \right]. \tag{8}$$

An equivalent expression holds for the outgoing path. For Auger processes, it has been demonstrated in Ref. [16] that the SCA is very accurate when calculating atomic occupancies.

Transition rates for different Auger processes contributing to neutralization of He^+ on Al were presented in Ref. [10], where the rates for direct Auger neutralization (from Ref. [17]) and direct Auger deexcitation were calculated using a surface response function; the process of indirect Auger deexcitation was found to be negligible. It should be noted that Ref. [10] dealt with Auger neutralization of He^+ at very low velocities (perpendicular energies smaller than a few eV) and therefore the calculation of the Auger rates made use of the following approximations: (i) the energy variation of the He-1*s* level with distance to the surface was not taken into account, since at very low velocities the ion is almost completely neutralized at very large distances when approaching the surface (at distances of ca. 3 a.u.); (ii) bulk plasmon assisted neutralization was neglected, since bulk plasmons cannot be excited at large distances from the surface. In the present case we deal with ion energies in the range 100–1000 eV, where He^+ can get close to the surface and variations of the He-1*s* level may become important. Moreover, in the present case the ion penetrates the jellium edge and its potential energy allows excitation of bulk plasmons, which is an important contribution to the Auger transition rate. Therefore in this work we will approach the Auger problem from a different perspective: the distance-dependent rate $1/\tau_{AC}(z)$ is calculated as the Auger capture rate of one electron to the adiabatic level $E_{1s}(z)$, using the bulk formula [18], valid for ion velocities much smaller than the Fermi velocity,

$$\frac{1}{\tau_{AC}(z)} = 2 \sum_{\mathbf{k}<k_F} \int_0^{\infty} d\omega \int \frac{d\mathbf{q}}{(2\pi)^3} \mathrm{Im} \frac{-1}{\epsilon_L(q,\omega)} \times |M(\mathbf{k},\mathbf{q})|^2 \delta(E_k - E_{1s}(z) - \omega), \tag{9}$$

with

$$M(\mathbf{k},\mathbf{q}) = \langle \psi_{\mathbf{k}} | e^{i\mathbf{q}\cdot\mathbf{r}} | \psi_{1s} \rangle. \tag{10}$$

In Eqs. (9) and (10), $\langle \mathbf{r} | \psi_{\mathbf{k}} \rangle$ is the wave function of a metal electron of momentum $\mathbf{k}$ and energy $E_{\mathbf{k}}$, k_F is the Fermi momentum, $\langle \mathbf{r} | \psi_{1s} \rangle$ is the atomic wave function and $\epsilon_L(q,\omega)$ is the Lindhard dielectric function. In calculating the matrix elements of Eq. (10) we have to take into account that E_{1s} is the energy of the He-1*s* level resulting from its interaction with the metal-core electrons. Therefore $|\psi_{1s}\rangle$ should be written as the linear combination,

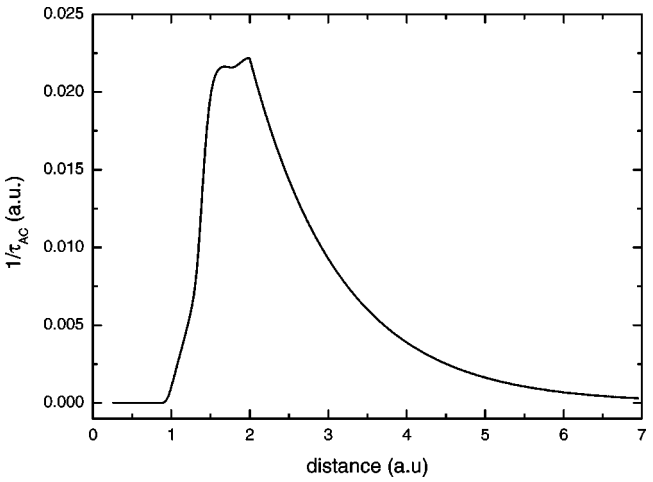

FIG. 5. The Auger capture rate for He on Al as a function of the distance to the surface.

$$|\psi_{1s}\rangle = c_{\mathrm{He}} |\psi_{\mathrm{He}}\rangle + \sum_l c_l |\psi_l\rangle, \tag{11}$$

where $\langle \mathbf{r} | \psi_{\mathrm{He}} \rangle$ is the He-1*s* wave function, $\langle \mathbf{r} | \psi_l \rangle$ is the wave function of the l-core orbital, and the coefficients c_{He} and c_l are known functions of the distance. When substituting Eq. (11) into Eq. (10) all the terms $\langle \psi_{\mathbf{k}} | e^{i\mathbf{q}\cdot\mathbf{r}} | \psi_l \rangle$ can be neglected, since the wave functions of the core levels are highly localized and we get

$$M(\mathbf{k},\mathbf{q}) = c_{\mathrm{He}} \langle \psi_{\mathbf{k}} | e^{i\mathbf{q}\cdot\mathbf{r}} | \psi_{\mathrm{He}} \rangle. \tag{12}$$

Finally, in Eq. (12) $|\psi_{\mathbf{k}}\rangle$ is taken as a plane wave orthogonalized to $|\psi_{\mathrm{He}}\rangle$ and for $\langle \mathbf{r} | \psi_{\mathrm{He}} \rangle$ we use a variational wave function of the He atom.

This calculation is carried out for distances z smaller than the jellium edge z_j ($z_j = 2$ a.u. for Al). For distances larger than z_j the Auger capture rate is assumed to decay exponentially as

$$\frac{1}{\tau_{AC}(z)} = \frac{1}{\tau_{AC}(z_j)} e^{-(z-z_j)/d_A}, \tag{13}$$

with $d_A = 1.15$ a.u. taken from Ref. [10]. As mentioned above, this effective distance was calculated using a surface dielectric function. The values of $1/\tau_{AC}$ are shown in Fig. 5. The rapid decrease of $1/\tau_{AC}$ for short distances is mainly due to the quick promotion of the adiabatic E_{1s} level. Note that the Auger rate becomes very small for distances shorter than ~ 1 a.u. where resonant processes set in, thus the spatial separation of Auger and resonant processes is actually realized. The Auger capture rate reaches its maximum at the jellium edge. This value is about a factor of 2 larger than the maximum value of $1/\tau_{AC}$ calculated in [17], the difference being mostly due to the contribution of the plasmon-assisted neutralization process. Another sophisticated calculation of the Auger capture rate was performed by Cazalilla *et al.*

[19]. These authors analyze the effects of an improved description of the He-1*s* wave function, which is more extended than the simplest variational wave function used in [17] and also in this work, and of the excited states of He. In their calculation, however, the He-1*s* energy level was assumed to be always shifted up by the image potential with a saturation at 4 eV. With these assumptions, the contribution of plasmon-assisted neutralization was ruled out. As a result, a net increase of the Auger rate by $50-100\,\%$ was obtained with respect to the earlier results of [17] in the range of distances near the image plane. This range of distances is relevant for experiments at grazing incidence, where the perpendicular energy of He is only of a few eV. In this regime, experiments have been performed by Hecht *et al.* [20], measuring neutralization of He^+. These authors deduced Auger transition rates from their experimental data and obtained, as a result, Auger rates that exceed the theoretical ones by two orders of magnitude, assuming that the neutralizing transition occurs at large distances from the surface where the use of a pure image potential shift of the He-1*s* level is justified. van Someren *et al.* [21] also performed experiments at grazing incidence, measuring electron-emission spectra. The spectra could be nicely reproduced by using the calculated He-1*s* level of Ref. [22] and either of the Auger rates calculated in [17] and [19]. Concerning the analysis of Ref. [20] van Someren showed that Auger rates close to the theoretical ones are deduced also from those data, if the theoretical He-1*s* energy is used as input data. Thus, the discrepancy between the Auger rates of Hecht *et al.* and theoretical ones could be traced back to the fact that Auger neutralization occurs also at distances where the image potential shift is not a realistic model for the position of the He-1*s* level. In summary, the comparison of theory to experiment gives confidence to the theoretical results for the position of the He level and the Auger rates.

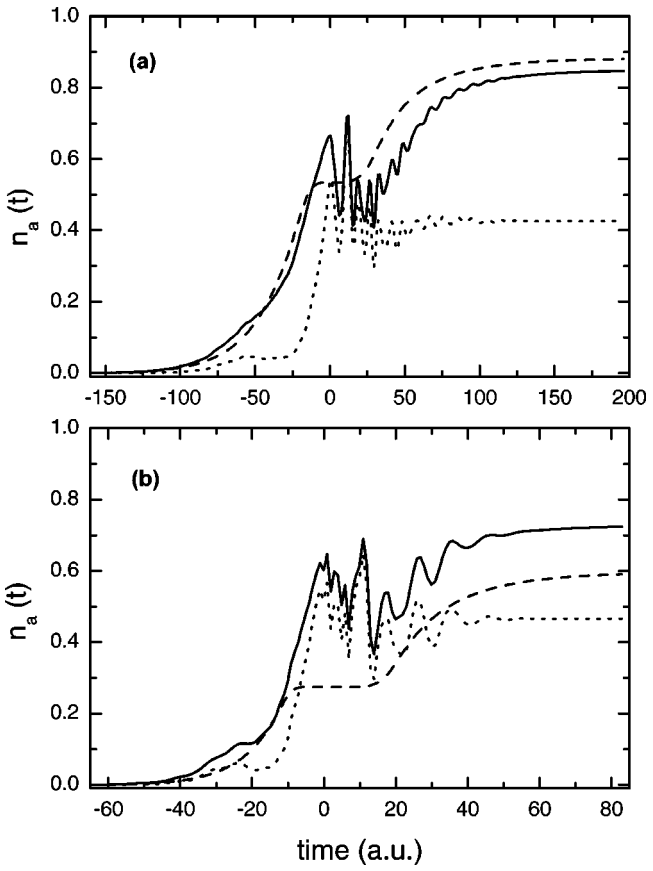

FIG. 6. The occupancy of the He-1*s* level interacting with Al as a function of the interaction time; $t=0$ corresponds to the turning point of the trajectory. Different lines show the results of calculations assuming: only resonant processes (dotted line), only Auger processes (dashed line), and Auger and resonant processes included together into the dynamic equation (continuous line). Ion incident energies of 260 eV in (a) and 1440 eV in (b).

V. RESULTS

In our resonant dynamic calculations we have chosen the ion trajectory and the velocities as discussed in Sec. II; for the diabatic $\tilde{E}_{1s}$ level we have used the values calculated in Sec. III for *both* the incoming and outgoing trajectories: for the outgoing trajectory we take $\tilde{E}_{1s}$ to depend on the metal atom-ion distance as shown in Figs. 2 (Al) and 4 (Pd). This approximation is valid if the resonant process is operative at very small distances only (below 3 a.u.), a region for which $\tilde{E}_{1s}$ is mainly determined by the binary interaction between the metal atom and the ion (see below).

Figure 6 shows the ion occupancy $n_{1s}(t)$ as a function of the trajectory timing; where $t=0$ corresponds to the turning point of the trajectory. We should mention that the turning point of the trajectory is a function of the ion kinetic energy and is calculated using $E[\mathrm{He}^+]$; to use $E[\mathrm{He}^0]$ for calculating the turning points would increase their values only by ca. 0.05 a.u., not introducing significant changes in $n_{1s}(t)$. From Fig. 6 we see that the resonant charge-exchange processes are localized around the turning point, at distances that do not depend strongly on the ion velocity. Thus, for $v=0.12$ a.u.(1.44 keV), this region extends up to ca. 2.5 a.u. and it does not significantly change down to $v=0.051$ a.u.(260 eV). In Fig. 6 we also include the values of $n_{1s}(t)$ calculated assuming Auger processes to be the only neutralization mechanism. Thus we see, how—along the incoming trajectory—Auger neutralization starts to operate at large distances, while resonant neutralization becomes important at small distances. This validates the approximation introduced in Sec. II to calculate P^+. In order to find a quantitative answer to the question of how good the ansatz of spatial separation of the processes is, we performed a dynamic calculation where Auger and resonant processes are treated simultaneously. This is done by using the dynamic Eq. (4) with the self-energy $\Sigma^r_{1s,1s}$ corrected by a term $(i/\tau_{AC})\delta(t-t_1)$. As a result we find that this ''local'' approximation to the Auger self-energy is a good one for calculating the atomic occupancy, for details see Ref. [16]. In Fig. 6 we also include $n_{1s}(t)$ as calculated using this dynamic approach. An important result of this analysis is that the final ion charge is accurately approximated by our calculation using Eq. (1).

In Figures 7 and 8 we show our calculated ion fractions P^+ for the He/Al and He/Pd systems together with experi-

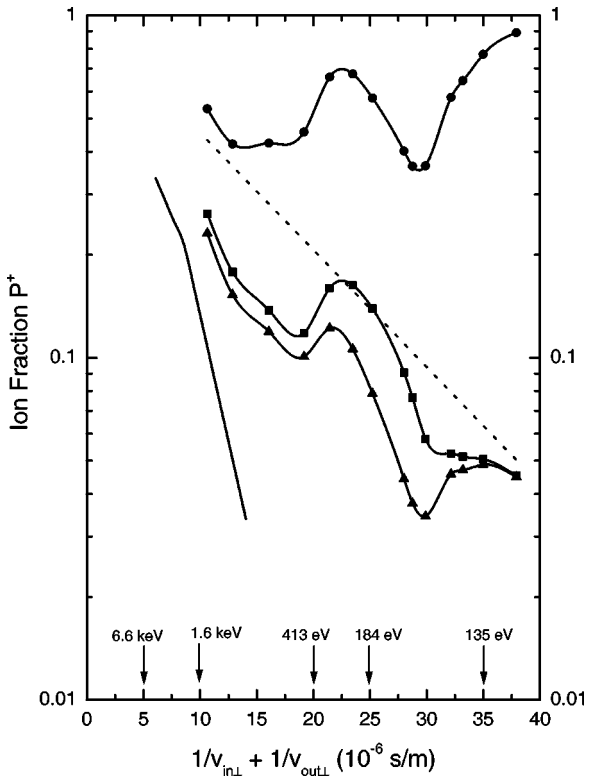

FIG. 7. The contribution of different processes to the ion fraction of He^+ backscattered from Al. Dashed line: Auger survival probability. Full circles: survival probability including resonant processes only. Full triangles: the results for the survival channel. Full squares: our full calculation for the ion fraction, obtained as the addition of the survival and reionization channels. The experimental data are shown by a continuous line. Incident energies are marked by arrows on the *x* axis.

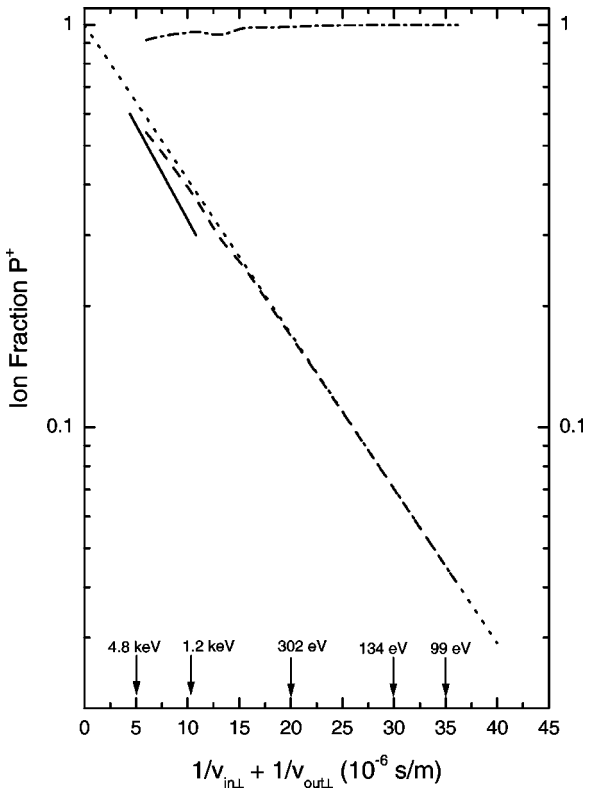

FIG. 8. The contribution of different processes to the ion fraction of He^+ backscattered from Pd. Dashed line: Auger survival probability. Dashed-dotted line: survival probability including resonant processes only. Long-dashed line: our full calculation for the ion fraction, obtained as the addition of the survival and reionization channels. The experimental data are shown by a continuous line. Incident energies are marked by arrows on the *x* axis.

mental data from Refs. [23] and [24] (bold lines). The various theoretical curves correspond to the following cases: P^+ assuming only resonant processes (P^+_{surv}), P^+ assuming only Auger processes ($P^+_{A,in}P^+_{A,out}$), and P^+ for the survival channel and our final result for P^+ as given by Eq. (1). Comparing the He/Al and the He/Pd results we find an important difference: for Al, resonant processes present a threshold at about 150 eV ion kinetic energy, while for Pd this threshold appears at about 1 keV. Moreover, for Al, resonant processes are found to be important in the region 150 eV$-$1.5 keV, contributing substantially to the total P^+, while for Pd the importance of resonant processes seems to be small, with a non-negligible contribution to P^+ only for ion energies between 1 and 4 keV.

VI. DISCUSSION AND CONCLUSIONS

The dynamic Eq. (4) for resonant processes can be fairly well approximated by using the adiabatic levels E_{1s} instead of the diabatic $\tilde{E}_{1s}$, and by including only effective hopping terms between the He-1*s* level and the conduction band. E_{1s} and $\tilde{E}_{1s}$ differ considerably (see Figs. 2 and 4), since the adiabatic level E_{1s} is promoted by its interaction with the metal-atom-core orbitals, and becomes resonant with the metal conduction band. This is the crucial point that makes the resonant processes operative. Thus it seems convenient to speak of ''collision-induced resonant neutralization'' rather than just of RN in this case.

Comparing our results for Al and for Pd, we find some important differences between the neutralization behavior of Al and Pd: while for Al the adiabatic level E_{1s} level resonates with the metal band at a metal-ion distance of $\sim$1 a.u., this resonance appears for Pd at distances of $\sim$2 a.u., making the charge-transfer processes between He^+ and Pd less effective.

Our final results for P^+ for the He/Al system shows an unusual behavior in the energy range 110 eV$-$1.5 keV, with two minima in the ion fraction around 150 eV and 400 eV kinetic energies. These two minima are due to resonant processes and can be traced back to the behavior of the hopping integral $T_{1s,3s}$ (see Fig. 1), which shows a pronounced minimum at $d\sim2$ a.u. and a negative slope in the range $\sim$0.5$-$2 a.u.; setting arbitrarily $T_{1s,3s}$ constant in the interval 0 to 2 a.u., we obtain a broad peak between 1.5 keV and 120 eV with just a minimum in P^+ for the resonant processes. These results show that the energy regime 260$-$120 eV represents a transition regime where resonant processes become important, leading to oscillations of P^+ and finally to an increase of P^+, once the resonant channel is fully open. Note that the

experimental data shown in Figs. 7 and 8 do not show any oscillations, as has to be expected since these experiments were performed in a rather narrow energy range.The system He/Al was analyzed also in Ref. [25]. The main differences between the results presented in Ref. [25] and the results of Fig. 7 are due to the inclusion of the Al-2*s* orbital, which was neglected in Ref. [25], and makes an important contribution to the promotion of the He-1*s* level.

Regarding the He/Pd system we summarize that, in this case the influence of resonant processes seems to be very small, so that neutralization is almost exclusively due to Auger processes. In other words, this is a system where Hagstrum's exponential law appears to be practically valid.

In summary, we find qualitative agreement comparing our calculations to experimental data. This is a satisfactory result, taking into account that our theory is a complex *ab initio* calculation, free of adjustable parameters. The following example may illustrate this situation: we would find an increase in the Auger rate $1/\tau_{AC}$ by 50%—and, equivalently, an increase in the matrix elements of Eq. (12) by around 20%—by just using a different set of orthogonalized wave functions when calculating Eq. (12), as found in Ref. [19]. Nevertheless, we decided to stay with the simpler single-ζ wave functions, since our main aim is rather to gain insight into the interplay of the relevant physical processes than to look for a quantitative description of experimental data.

ACKNOWLEDGMENTS

We are indebted to P. Pou, F. J. García Vidal, R. Pérez, and J. Ortega for useful discussions. This work has been funded by the Spanish Comisión Interministerial de Ciencia y Tecnología under Contracts No. PB97-0044 and PB97-0028. E.A.G. and N.P.W. acknowledge the Spanish Comisión Interministerial de Ciencia y Tecnología for financial support. E.A.G. was also finally supported by Consejo Nacional de Investigaciones Científicas y Técnicas (CONICET, Argentina) and Fundación Antorchas (Argentina) under Contract No. A-13564/1-26.

[1] H.H. Brongersma, P.A.C. Groenen, and J.-P. Jacobs, in *Science of Ceramic Interfaces II*, Materials Science Monographs Vol. 81, edited by J. Nowotny (Elsevier, New York, 1994), p. 113.
[2] H.D. Hagstrum, Phys. Rev. **96**, 336 (1954).
[3] A. Blandin, A. Nourtier, and D.W. Hone, J. Phys. (Paris) **37**, 369 (1976).
[4] R. Brako and D.M. Newns, Surf. Sci. **108**, 253 (1981).
[5] J.J.C. Geerlings and J. Los, Phys. Rep. **190**, 133 (1990).
[6] Evelina A. García, E.C. Goldberg, and M.C.G. Passeggi, Surf. Sci. **325**, 311 (1995).
[7] J. Merino, N. Lorente, P. Pou, and F. Flores, Phys. Rev. B **54**, 10959 (1996).
[8] S. Tsuneyuki and M. Tsukada, Phys. Rev. B **34**, 5758 (1986).
[9] Evelina A. García, P.G. Bolcatto, and E.C. Goldberg, Phys. Rev. B **52**, 16924 (1995).
[10] W. More, J. Merino, R. Monreal, P. Pou, and F. Flores, Phys. Rev. B **58**, 7385 (1998).
[11] D. A. Papaconstantopoulos, *Handbook of the Band Structure of the Elemental Solids* (Plenum Press, New York, 1986).
[12] E. Clementi and C. Roetti, At. Data Nucl. Data Tables **14**, 177 (1974).
[13] J. Fernández Rico, R. López, and G. Ramirez, J. Chem. Phys. **91**, 4204 (1989); **91**, 4213 (1989).
[14] J. Fernández Rico, R. López, and G. Ramirez, in *Studies in Physical and Theoretical Chemistry*, edited by S. Fraga (Elsevier Science, Amsterdam, 1992), Vol. 77 (A), p. 241.
[15] L.V. Keldysh, Zh. Éksp. Teor. Fiz. **47**, 1515 (1964) [Sov. Phys. JETP **20**, 1018 (1965)].
[16] Evelina A. García and R. Monreal, Phys. Rev. B **61**, 13565 (2000).
[17] N. Lorente and R. Monreal, Phys. Rev. B **53**, 9622 (1996); N. Lorente and R. Monreal, Surf. Sci. **370**, 324 (1997).
[18] P.M. Echenique, F. Flores, and R.H. Ritchie, in *Solid State Physics: Advances in Research and Applications*, edited by H. Ehrenreich and D. Turnbull (Academic Press, New York, 1990), Vol. 43, p. 229.
[19] M.A. Cazalilla, N. Lorente, R. Diez Muiño, J.-P. Gauyacq, D. Teillet-Billy, and P.M. Echenique, Phys. Rev. B **58**, 13991 (1998).
[20] T. Hecht, H. Winter, and A.G. Borisov, Surf. Sci. **406**, L607 (1998).
[21] B. van Someren, P.A. Zeijlmans van Emmichoven, and A. Niehaus, Phys. Rev. A **61**, 022902 (2000).
[22] J. Merino, N. Lorente, W. More, F. Flores, and M.Yu. Gusev, Nucl. Instrum. Methods Phys. Res. B **125**, 250 (1997).
[23] G.C. van Leerdam and H.H. Brongersma, Surf. Sci. **254**, 152 (1991).
[24] L.C.A. van den Oetelaar, S.N. Mikhailov, and H.H. Brongersma, Nucl. Instrum. Methods Phys. Res. B **45**, 420 (1994).
[25] E.C. Goldberg, R. Monreal, F. Flores, H.H. Brongersma, and P. Bauer, Surf. Sci. **440**, L875 (1999).